ACS APPLIED MATERIALS & INTERFACES

Letter

www.acsami.org

Low-Temperature Thermal Reduction of Graphene Oxide Nanobrick Walls: Unique Combination of High Gas Barrier and Low Resistivity in Fully Organic Polyelectrolyte Multilayer Thin Films

Bart Stevens,[†] Ekaterina Dessiatova,[†] David A. Hagen,[†] Alexander D. Todd,[‡] Christopher W. Bielawski,[‡] and Jaime C. Grunlan*[,†]

[†]Department of Mechanical Engineering, Texas A&M University, College Station, Texas 77843-3123, United States

[‡]Department of Chemistry and Biochemistry, The University of Texas at Austin, Austin, Texas 78712, United States

Supporting Information

ABSTRACT: Layer-by-layer assembly from aqueous solutions was used to construct multilayer thin films (<200 nm) comprising polyethylenimine and graphene oxide. Low-temperature (175 °C) thermal reduction of these films improved gas barrier properties (e.g., lower permeability than SiO_x), even under high humidity conditions, and enhanced their electrical conductivity to 1750 S/m. The flexible nature of the aforementioned thin films, along with their excellent combination of transport properties, make them ideal candidates for use in a broad range of electronics and packaging applications.

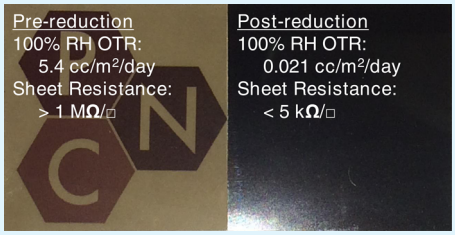

KEYWORDS: *layer-by-layer assembly, oxygen barrier, thin films, reduced graphene oxide, sheet resistance*

Strong interest in traditional (and flexible) organic electronics is driving the need for electrically conductive layers with high oxygen barrier properties that can be applied using low-cost methods.[1,2] Commercially available options for surface coatings that meet these requirements rely on expensive vapor phase application under vacuum,[3] such as SiO_x, Al_xO_y, and metallized films, which are subject to cracking and pinhole defects.[4,5] Although graphene, a single layer flake of sp^2 carbon atoms, can be difficult to work with because of high van der Waals interactions,[6] graphene oxide (GO, a graphene-like material functionalized with epoxide, hydroxyl, carboxyl groups) is amenable to aqueous processing.[7] Although both graphene and GO have been found suitable for their impermeability to a variety of gases,[8,9] the latter is an electrical insulator. Electrical conductivity can be enhanced by chemical or thermal reduction to form reduced graphene oxide (rGO), which often displays properties necessary for flexible electronics.[10,11] The multipurpose nature of graphene oxide, combined with the straightforward layer-by-layer process, creates an opportunity for inexpensive application for electronics packaging and other types of encapsulation.

Layer-by-layer (LbL) assembly is a thin film deposition technique that relies on exposing a substrate to alternating aqueous solutions of oppositely charged polyelectrolytes.[12,13] This technique has been used to prepare films that display a range of applications, including drug delivery,[14,15] sensing,[16] self-cleaning,[17] and flame retardancy.[18] The thickness and morphology of the deposited layers may be tuned by varying processing conditions (e.g., pH[19] and concentration[20]) of the requisite solutions, which ultimately influences macroscopic properties such as gas permeability.[21,22] Graphene oxide has been shown to display gas barrier[9] and electrical conductivity (upon reduction),[23,24] when applied using LbL processing, but the barrier properties were not retained under humid conditions and electrical conductivity required exposure to toxic chemicals (e.g., hydrazine). When heated to 175 °C in air for 90 min, graphene oxide undergoes reduction and, in a multilayer assembly with polyethylenimine, displays both low sheet resistance (<5 kΩ/□) and oxygen permeability (e.g., the oxygen transmission rate is 3−4 orders of magnitude lower than uncoated poly(ethylene terephthalate)) under dry as well as humid conditions. The extent of GO reduction, and hence electrical resistance and gas permeability, may be tuned by varying the temperature and exposure time.

Thin film growth was achieved with an aqueous polyethylenimine (PEI) solution (0.1 wt % at pH 10) and aqueous graphene oxide (GO) suspension (0.1 wt % at pH 3.3) through an alternating deposition sequence on 175 μm PET film. As illustrated in Figure 1a, this layer-by-layer process resulted in anion−cation bilayers on the substrate through the formation of electrostatic interactions. Profilometry was used to monitor the thickness of these films, both as-prepared and after thermally reducing the films at 175 °C for 90 min, as shown in Figure 1b.

At 20 bilayers, the film thickness was approximately 173 nm, as measured on silicon, although thermal reduction reduces this value to 120 nm (i.e., 70% of original thickness). Additionally, the coverage of GO was uniform across the assembly, and the observed wrinkling of GO platelets diminished upon reduction (Figure 2a, b). The TEM images indicated that GO platelets

Received: May 14, 2014
Accepted: June 20, 2014
Published: June 20, 2014

   dx.doi.org/10.1021/am502889w | *ACS Appl. Mater. Interfaces* 2014, 6, 9942−9945

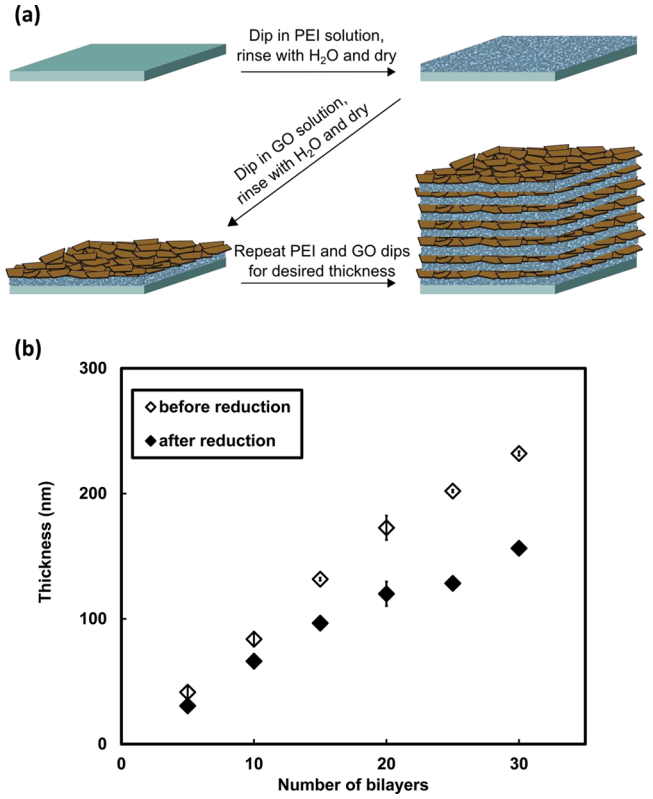

Figure 1. (a) Schematic of layer-by-layer deposition of polyethylenimine and graphene oxide bilayers onto a substrate and (b) profilometer thickness of PEI/GO assemblies grown on silicon before and after reduction at 175 °C for 90 min.

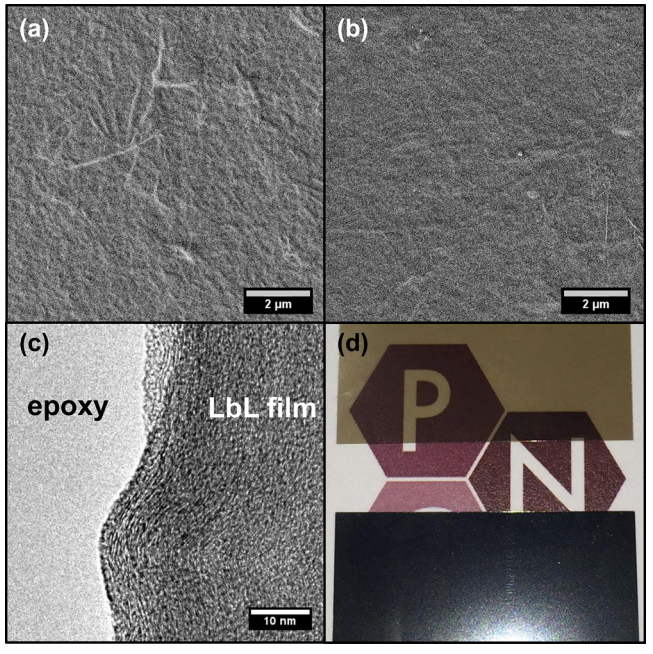

Figure 2. SEM micrographs of 20 bilayer PEI/GO assemblies (a) before and (b) after 90 min thermal reduction at 175 °C. TEM micrograph of the same thin film before reduction (c), showing GO oriented parallel to the film. Thermal reduction of a 10-bilayer assembly results in the originally transparent film (d, top) becoming opaque, with a graphitic luster (d, bottom).

were aligned parallel to the direction of the substrate and packed closely together (Figure 2c). Although the density of graphene oxide appeared to be high, the film was optically transparent until it was thermally reduced (Figure 2d), at which point the film obtains a metallic luster similar to that of graphite. A more detailed description of materials, procedures, and characterization used in this study can be found in the Supporting Information.

Thermal reduction of GO was monitored by electrical conductivity and X-ray photoelectron spectroscopy (XPS) measurements. In the most reduced state, the PEI/GO films exhibited a decrease in electrical sheet resistance by more than 4 orders of magnitude. Four-point probe resistivity measurements indicated that electrical sheet resistance decreased from $>1 \times 10^7$ Ω/□ to 4760 Ω/□ following a 90 min reduction at 175 °C (in an ambient atmosphere), corresponding to a conductivity of 1750 S/m. Increased electrical conductivity was the result of partial restoration of sp^2 carbon bonds in the reduced GO. XPS revealed a decrease in C 1s peak intensity at 286.5 eV, relative to 284.5 eV (Figure 3), indicative of fewer C−O bonds and higher sp^2 carbon content characteristic of graphite.[25]

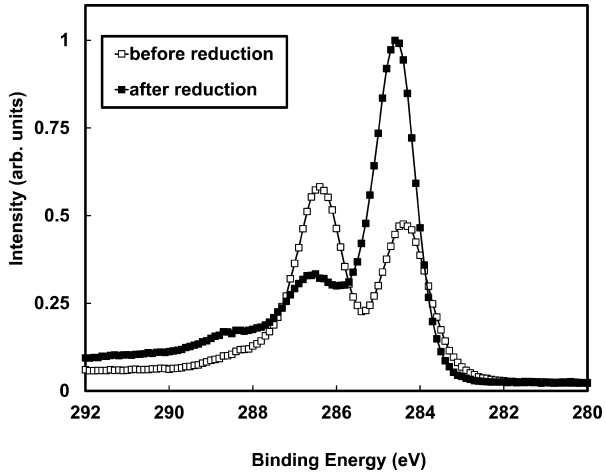

Figure 3. C 1s XPS spectrum of graphene oxide before and after a 90 min reduction at 175 °C. The increase in peak intensity at 284 eV, relative to 286 eV, after reduction reflects partial restoration of the graphitic character of GO.

It is important to note that the reduction conditions used for these PEI/GO assemblies on 175 μm thick, commercial-grade PET were mild, and no loss of film or substrate integrity was observed by SEM. Because these assemblies displayed a continuum of electrical resistivities between their prereduced and maximally reduced states (Figure 4), it is apparent that the degree of reduction may be tailored, along with the associated properties.

Table 1 summarizes the oxygen barrier properties of these assemblies, which were measured with oxygen transmission rate (OTR) testing of coated PET samples, in both 0% (dry) and 100% (humid) relative humidity conditions. Prior to thermal reduction, the GO/PEI multilayer thin films displayed excellent barrier properties to oxygen under dry conditions; indeed, with as few as 10 bilayers, dry OTR decreased from 8.6 to 0.0078 cc m^{-2} day^{-1} atm^{-1}. Depositing 20 PEI/GO bilayers caused the OTR to drop below the detection limit of commercial instrumentation (<0.005 cc m^{-2} day^{-1} atm^{-1}).[26] When a 90

dx.doi.org/10.1021/am502889w | ACS Appl. Mater. Interfaces 2014, 6, 9942−9945

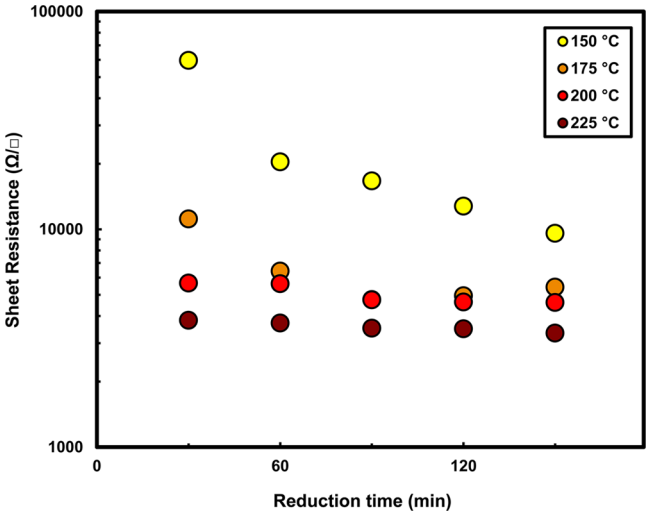

Figure 4. Sheet resistance as a function of exposure time, for 20 bilayer PEI/GO assemblies, to various thermal reduction temperatures (see legend). The standard deviation for the five measurements taken for each data point is smaller than the size of the markers for the points.

min thermal reduction at 175 °C was applied to these 10 and 20 bilayer assemblies, both exhibited OTR values below detection. Reduction of the GO decreased 10 bilayer film permeability from 15 to <7.0 × 10^{-22} $cm^2/Pa/s$,[27] a value comparable to the lowest reported dry oxygen film permeability measured for an LbL film.[28]

Under humid conditions, prereduced and reduced assemblies show a wide disparity. With 20 bilayers deposited, the OTR of GO/PEI exhibited little improvement over bare PET, decreasing by less than a factor of 2. When thermally reduced, the humid OTR of the resulting rGO/PEI assemblies decreased to 0.98 and 0.022 cc m^{-2} day^{-1} atm^{-1} for 10 and 20 bilayer films, respectively. Although the OTR barrier observed in dry conditions was not fully realized in humid conditions, these assemblies reduced oxygen transmission substantially better than bare PET. GO-based assemblies have displayed a propensity for dry oxygen barrier applications,[9] but humid oxygen barrier has been difficult to achieve due to the hydrophilic nature of the assemblies that leads to swelling and increased permeability.[29,30] Compaction of PEI/GO assemblies upon reduction effectively increased the nanoplatelet concentration, and hydrophilic GO was transformed into hydrophobic rGO, which likely inhibits film swelling.

Nanocoatings with high conductivity and low oxygen permeability are very desirable for electronics packaging applications.[1,2] Ambient processing from aqueous solutions provides a simple and cost-effective route to graphene oxide-based thin films with these properties. Relatively low temperature (<200 °C) treatment in air affords the ability to improve electrical sheet resistance and decrease film permeability. The increased hydrophobicity of the reduced thin film results in decreased permeability that is retained at high humidity. Collectively, the exceptional functionality and flexible nature of these coatings, along with the ease with which they are applied, makes them ideal for use in a variety of electronics packaging and encapsulation applications.

■ ASSOCIATED CONTENT

Ⓢ Supporting Information

Experimental procedures for formation of graphene oxide and layer-by-layer assemblies, as well as spectroscopic information and descriptions of methods used to characterize these thin films. This material is available free of charge via the Internet at http://pubs.acs.org/.

■ AUTHOR INFORMATION

Corresponding Author

*E-mail: jgrunlan@tamu.edu.

Funding

This work was funded by United States Air Force Office of Scientific Research Grant FA9550-09-1-0609 and National Science Foundation Grant CHE-1266323.

Notes

The authors declare no competing financial interest.

■ ACKNOWLEDGMENTS

The authors from Texas A&M acknowledge the United States Air Force Office of Scientific Research (Grant FA9550-09-1-0609), under the auspices of Dr. Charles Lee, for financial support of this work. The authors from the University of Texas at Austin are grateful to the NSF (CHE-1266323) for their financial support. Use of the TAMU Microscopy and Imaging Center and the Materials Characterization Facility is also acknowledged.

■ REFERENCES

(1) Lupinski, J. H.; Moore, R. S. Polymeric Materials for Electronics Packaging and Interconnection - an Overview. *ACS Symp. Ser.* **1989**, *407*, 1−25.

Table 1. Oxygen Transmission Rate and Permeability Data for GO/PEI Assemblies on PET, before and after a 90 min Thermal Reduction at 175 °C

system		film thickness (nm)	relative humidity (%)	OTR (cc m^{-2} day^{-1} atm^{-1})	total permeablility (× 10^{-15} cm^2 /(Pa/s))	LbL film permeability[27] (× 10^{-18} cm^2 /(Pa/s))
bare PET				8.6	1.7	
10 BL	unreduced	84	0	0.0078	0.0016	0.0015
	reduced	66	0	<0.0047	<0.000 95	<0.000 70
	unreduced	84	100	5.8	1.2	3.3
	reduced	66	100	0.98	0.20	0.17
20 BL	unreduced	173	0	<0.0047	<0.000 95	<0.0018
	reduced	120	0	<0.0047	<0.000 95	<0.0013
	unreduced	173	100	5.4	1.1	5.8
	reduced	120	100	0.022	0.0044	0.0060

(2) Lewis, J. S.; Weaver, M. S. Thin-Film Permeation-Barrier Technology for Flexible Organic Light-Emitting Devices. *IEEE J. Sel. Top. Quantum Electron.* **2004**, *10*, 45−57.
(3) Kamp, M.; Bartsch, J.; Nold, S.; Retzlaff, M.; Horteis, M.; Glunz, S. W. Economic Evaluation of Two-Step Metallization Processes for Silicon Solar Cells. *Energy Procedia* **2011**, *8*, 558−564.
(4) Yanaka, M.; Henry, B. M.; Roberts, A. P.; Grovenor, C. R. M.; Briggs, G. A. D.; Sutton, A. P.; Miyamoto, T.; Tsukahara, Y.; Takeda, N.; Chater, R. J. How Cracks in SiOx-Coated Polyester Films Affect Gas Permeation. *Thin Solid Films* **2001**, *397*, 176−185.
(5) Mercea, P.; Muresan, L.; Mecea, V. Permeation of Gases through Metallized Polymer Membranes. *J. Membr. Sci.* **1985**, *24*, 297−307.
(6) Li, D.; Muller, M. B.; Gilje, S.; Kaner, R. B.; Wallace, G. G. Processable Aqueous Dispersions of Graphene Nanosheets. *Nat. Nanotechnol.* **2008**, *3*, 101−105.
(7) Dreyer, D. R.; Park, S.; Bielawski, C. W.; Ruoff, R. S. The Chemistry of Graphene Oxide. *Chem. Soc. Rev.* **2010**, *39*, 228−240.
(8) Bunch, J. S.; Verbridge, S. S.; Alden, J. S.; van der Zande, A. M.; Parpia, J. M.; Craighead, H. G.; McEuen, P. L. Impermeable Atomic Membranes from Graphene Sheets. *Nano Lett.* **2008**, *8*, 2458−2462.
(9) Yang, Y. H.; Bolling, L.; Priolo, M. A.; Grunlan, J. C. Super Gas Barrier and Selectivity of Graphene Oxide-Polymer Multilayer Thin Films. *Adv. Mater.* **2013**, *25*, 503−508.
(10) El-Kady, M. F.; Strong, V.; Dubin, S.; Kaner, R. B. Laser Scribing of High-Performance and Flexible Graphene-Based Electrochemical Capacitors. *Science* **2012**, *335*, 1326−1330.
(11) Eda, G.; Fanchini, G.; Chhowalla, M. Large-Area Ultrathin Films of Reduced Graphene Oxide as a Transparent and Flexible Electronic Material. *Nat. Nanotechnol.* **2008**, *3*, 270−274.
(12) Decher, G.; Schlenoff, J. B. *Multilayer Thin Films: Sequential Assembly of Nanocomposite Materials*, 2nd rev. ed..; Wiley-VCH: Weinheim, Germany, 2012.
(13) Ariga, K.; Ji, Q.; Hill, J. P.; Bando, Y.; Aono, M. Forming Nanomaterials as Layered Functional Structures toward Materials Nanoarchitectonics. *NPG Asia Mater.* **2012**, *4*, 11.
(14) Caridade, S. G.; Monge, C.; Gilde, F.; Boudou, T.; Mano, J. F.; Picart, C. Free-Standing Polyelectrolyte Membranes Made of Chitosan and Alginate. *Biomacromolecules* **2013**, *14*, 1653−60.
(15) Poon, Z.; Lee, J. B.; Morton, S. W.; Hammond, P. T. Controlling in Vivo Stability and Biodistribution in Electrostatically Assembled Nanoparticles for Systemic Delivery. *Nano Lett.* **2011**, *11*, 2096−103.
(16) Robert, C.; Feller, J. F.; Castro, M. Sensing Skin for Strain Monitoring Made of PC-CNT Conductive Polymer Nanocomposite Sprayed Layer by Layer. *ACS Appl. Mater. Interfaces* **2012**, *4*, 3508−3516.
(17) Shen, L.; Wang, B.; Wang, J.; Fu, J.; Picart, C.; Ji, J. Asymmetric Free-Standing Film with Multifunctional Anti-Bacterial and Self-Cleaning Properties. *ACS Appl. Mater. Interfaces* **2012**, *4*, 4476−83.
(18) Laufer, G.; Kirkland, C.; Morgan, A. B.; Grunlan, J. C. Exceptionally Flame Retardant Sulfur-Based Multilayer Nanocoating for Polyurethane Prepared from Aqueous Polyelectrolyte Solutions. *ACS Macro Lett.* **2013**, *2*, 361−365.
(19) Shiratori, S. S.; Rubner, M. F. pH-Dependent Thickness Behavior of Sequentially Adsorbed Layers of Weak Polyelectrolytes. *Macromolecules* **2000**, *33*, 4213−4219.
(20) Garg, A.; Heflin, J. R.; Gibson, H. W.; Davis, R. M. Study of Film Structure and Adsorption Kinetics of Polyelectrolyte Multilayer Films: Effect of pH and Polymer Concentration. *Langmuir* **2008**, *24*, 10887−10894.
(21) Priolo, M. A.; Holder, K. M.; Gamboa, D.; Grunlan, J. C. Influence of Clay Concentration on the Gas Barrier of Clay-Polymer Nanobrick Wall Thin Film Assemblies. *Langmuir* **2011**, *27*, 12106−12114.
(22) Priolo, M. A.; Gamboa, D.; Grunlan, J. C. Transparent Clay-Polymer Nano Brick Wall Assemblies with Tailorable Oxygen Barrier. *ACS Appl. Mater. Interfaces* **2010**, *2*, 312−320.
(23) Kotov, N. A.; Dekany, I.; Fendler, J. H. Ultrathin Graphite Oxide-Polyelectrolyte Composites Prepared by Self-Assembly: Transition between Conductive and Non-Conductive States. *Adv. Mater.* **1996**, *8*, 637−641.
(24) Zhu, J. Y.; He, J. H. Assembly and Benign Step-by-Step Post-Treatment of Oppositely Charged Reduced Graphene Oxides for Transparent Conductive Thin Films with Multiple Applications. *Nanoscale* **2012**, *4*, 3558−3566.
(25) Larciprete, R.; Fabris, S.; Sun, T.; Lacovig, P.; Baraldi, A.; Lizzit, S. Dual Path Mechanism in the Thermal Reduction of Graphene Oxide. *J. Am. Chem. Soc.* **2011**, *133*, 17315−17321.
(26) OTR testing was performed by Mocon, Inc. The low end detection limit of the Ox Tran 2/21 L module is 0.00465 cc m^{-2} day^{-1}.
(27) Film permeability was decoupled from total permeability (the permeability of the film and substrate) as previously noted in reference 2.
(28) Priolo, M. A.; Gamboa, D.; Holder, K. M.; Grunlan, J. C. Super Gas Barrier of Transparent Polymer-Clay Multi Layer Ultrathin Films. *Nano Lett.* **2010**, *10*, 4970−4974.
(29) Wong, J. E.; Rehfeldt, F.; Hanni, P.; Tanaka, M.; Klitzing, R. V. Swelling Behavior of Polyelectrolyte Multilayers in Saturated Water Vapor. *Macromolecules* **2004**, *37*, 7285−7289.
(30) Nolte, A. J.; Treat, N. D.; Cohen, R. E.; Rubner, M. F. Effect of Relative Humidity on the Young's Modulus of Polyelectrolyte Multilayer Films and Related Nonionic Polymers. *Macromolecules* **2008**, *41*, 5793−5798.